

# Dilute helium solutions in particle-physics experiments: response to a heat source

Gordon Baym,<sup>a,b</sup> D. H. Beck,<sup>a</sup> and C. J. Pethick<sup>a,b,c</sup>

<sup>a</sup>*Department of Physics, University of Illinois, 1110 W. Green Street, Urbana, IL 61801*

<sup>b</sup>*The Niels Bohr International Academy, The Niels Bohr Institute,  
Blegdamsvej 17, DK-2100 Copenhagen Ø, Denmark*

<sup>c</sup>*NORDITA, KTH Royal Institute of Technology and Stockholm University, Roslagstullsbacken 23, SE-10691 Stockholm, Sweden*

(Dated: December 13, 2012)

Motivated by a proposed experimental search for the electric dipole moment of the neutron (nEDM) utilizing neutron- $^3\text{He}$  capture in a dilute solution of  $^3\text{He}$  in superfluid  $^4\text{He}$ , we reanalyze a measurement in a related system by Lamoreaux et al. of the  $^3\text{He}$  density distribution in a dilute solution in the presence of a heat flow. We show, from considering the thermodynamics and hydrodynamics of dilute solutions, that this experiment in fact measures the thermal conductivity of the solution. Calculating the thermal conductivity within a microscopic framework, taking into account phonon-phonon, phonon- $^3\text{He}$ , and  $^3\text{He}$ - $^3\text{He}$  scatterings, we find satisfactory agreement of theory with the data, serving to confirm our understanding of the microscopics of the helium in the nEDM experiment.

PACS numbers: 67.60.G- 13.40.Em

## I. INTRODUCTION

The proposed experiment [1] to measure the neutron electric dipole moment at the Oak Ridge National Laboratory Spallation Neutron Source (SNS) utilizes the absorption of ultracold polarized neutrons on polarized  $^3\text{He}$  atoms in solution in superfluid  $^3\text{He}$ , via the reaction



A crucial issue is to be able to periodically sweep out the  $^3\text{He}$  by means of heat pulses [2]; the underlying physics of the transport is scattering of phonons in the superfluid  $^4\text{He}$  against the  $^3\text{He}$ . A pioneering experiment by Lamoreaux et al. [3] (hereinafter referred to as I), measuring the effect of a heat source on the steady state distribution of  $^3\text{He}$  atoms in a dilute solution in superfluid  $^4\text{He}$ , provides a prototype for the effects of a phonon wind on the  $^3\text{He}$ .

The experiment described in I utilizes a novel technique to measure the thermal transport properties of dilute solutions. The solution is contained in a cylindrical cell roughly 5 cm in diameter and 5 cm long, cooled at one end by a dilution refrigerator to a temperature  $T$  in the range 0.45–0.95 K. The concentration of  $^3\text{He}$  in solution,  $x_3 = n_3/(n_3 + n_4)$ , where  $n_3$  and  $n_4$  are the  $^3\text{He}$  and  $^4\text{He}$  number densities, is in the range  $7 \times 10^{-5}$  to  $3 \times 10^{-4}$ . A temperature gradient is created by a resistive heater generating 7–15 mW, located roughly midway between the ends and near the cylinder wall (see Fig. 4 below). The resulting spatial distribution of the  $^3\text{He}$  density is probed by a well-collimated neutron beam of diameter  $\sim 0.25$  cm going through the cell. A fraction of the neutrons are captured via the reaction (1). The XUV scintillation light from protons and tritons in the liquid  $^4\text{He}$  is converted to visible light and detected by a photomultiplier tube which views the solution through a window at the other end of the cell. The yield of scintillation light,

measured as a function of cell temperature, initial  $^3\text{He}$  concentration, and heater power is used to determine the thermally induced change in the  $^3\text{He}$  distribution.

The experiment was originally analyzed in terms of diffusion of the  $^3\text{He}$  at fixed temperature, described by a diffusion constant. In this paper we reconsider the results of the experiment at low temperatures in terms of the full hydrodynamical description of dilute solutions of  $^3\text{He}$  and superfluid  $^4\text{He}$  [4]. In the temperature regime,  $T \lesssim 0.6$  K, on which we focus, phonons are the dominant excitations in the superfluid, and carry most of the heat. In the following section we lay out the basic thermodynamics and hydrodynamics of dilute solutions, and show that under stationary conditions in the relevant range of  $x_3$ , gradients of the  $^3\text{He}$  density are, in fact, accompanied by non-negligible temperature gradients. We conclude that the experiment measures the overall thermal conductivity of the solution, rather than the  $^3\text{He}$  diffusion constant.

The basic scattering mechanisms determining the transport properties of dilute solutions –  $^3\text{He}$ - $^3\text{He}$ ,  $^3\text{He}$ -phonon, and phonon-phonon interactions – are spelled out in Sec. III. In the concentration regime of the experiment in I, the  $^3\text{He}$ - $^3\text{He}$  interactions are sufficiently strong that they keep the  $^3\text{He}$  in thermal equilibrium at rest at the local temperature  $T(\vec{r})$ . The phonon-phonon interactions keep the phonon momentum distribution in equilibrium, drifting at a velocity  $\vec{v}_{ph}$ . In Sec. IV, we calculate the thermal conductivity (dominated by the phonons) in this situation, by considering the drag force on the phonons due to their scattering against the stationary  $^3\text{He}$ . The method we use is identical to that used in an earlier calculation of the mobility of ions in superfluid  $^4\text{He}$  [5], and later used by Bowley [6] in his accounting of the Lamoreaux et al. experiment. Our calculation of the momentum transfer between phonons and  $^3\text{He}$  agrees in structure with Bowley's calculation. In Sec. V, we relate the effective diffusion constant extracted in I to the

actual thermal conductivity of the dilute solutions, and show how the microscopic theory satisfactorily explains the experimental findings in I.

At lower  $^3\text{He}$  concentrations,  $x \lesssim 10^{-6}$ , the transport must be calculated by solving the coupled Boltzmann equations for the phonons and  $^3\text{He}$ ; the results will be given in [7]. Finally, the impact of these results on the transport of  $^3\text{He}$  in the much lower concentration regime of the SNS neutron electric dipole moment experiment will be described separately in a third paper [8].

## II. RESPONSE TO STATIC DISTURBANCES

To understand how dilute solutions of  $^3\text{He}$  in superfluid  $^4\text{He}$  respond to a localized static heat source, we first review the hydrodynamics of the solutions. At low temperatures the phonons are the dominant excitations of the  $^4\text{He}$ , and the momentum density or mass current density of the  $^4\text{He}$  is

$$\vec{g}_4 = \rho_s \vec{v}_s + \rho_{ph} \vec{v}_{ph}, \quad (2)$$

where  $\vec{v}_s$  is the superfluid flow velocity,  $\vec{v}_{ph}$  is the phonon fluid flow velocity,  $\rho_s$  is the superfluid mass density, and  $\rho_{ph} (\ll \rho_s)$  is the  $^4\text{He}$  normal fluid density. Similarly, the  $^3\text{He}$  momentum density is

$$\vec{g}_3 = \rho_3 \vec{v}_3, \quad (3)$$

where  $\vec{v}_3$  is the  $^3\text{He}$  flow velocity, and  $\rho_3 = m^* n_3$ , with  $m^* = m_3 + \delta m \simeq 2.34 m_3$  the effective mass [10]. The total mass current,  $\vec{g}$ , is  $\vec{g}_4 + \vec{g}_3$ .

When the  $^4\text{He}$  mass flow vanishes,  $|v_s| = (\rho_{ph}/\rho_s) v_{ph} \ll v_{ph}$  at temperatures  $\lesssim 0.6$  K, and thus in the absence of  $^3\text{He}$  mass flow, the only relevant flow velocity is that of the phonons. Then force balance in the dilute solutions implies that to linear order,

$$\nabla P = \eta_{ph} \nabla^2 \vec{v}_{ph}, \quad (4)$$

where  $P = P_3 + P_{ph}$  is the total pressure, with  $P_3 = n_3 T$  the  $^3\text{He}$  partial pressure (we generally work in units with  $\hbar$  and Boltzmann's constant,  $k_B$ , equal to unity),  $T$  is the temperature,  $P_{ph}$  is the phonon partial pressure, and  $\eta_{ph}$  the first viscosity of the normal fluid. In the experiment in I, the viscosity term is insignificant compared with the drag of the  $^3\text{He}$  on the phonons, as we show in Sec. IV. Thus the total pressure is effectively constant throughout the system. (However, at the ultralow  $^3\text{He}$  concentrations of the proposed SNS experiment, the phonon viscosity does play a significant role [8].)

In addition, as one sees from the linearized superfluid acceleration equation [9],

$$m_4 \frac{\partial \vec{v}_s}{\partial t} + \nabla \mu_4 = 0, \quad (5)$$

the  $^4\text{He}$  chemical potential,  $\mu_4$ , is also constant in a steady state. The Gibbs-Duhem relation for the solutions,  $\nabla P = n_4 \nabla \mu_4 + n_3 \nabla \mu_3 + S \nabla T$ , with  $\mu_3$  the  $^3\text{He}$

chemical potential,  $T$  the temperature, and  $S$  the total entropy density, then implies that

$$\nabla P_3 + S_{ph} \nabla T = 0, \quad (6)$$

where  $S_{ph} = 4P_{ph}/T$  is the phonon entropy density, and  $dP_{ph} = S_{ph} dT$ . Equation (6) then tells us the simple relation between the temperature and  $^3\text{He}$  density gradients

$$\nabla T = -\frac{T}{S_{ph} + n_3} \nabla n_3; \quad (7)$$

in a steady state a gradient of the  $^3\text{He}$  density is always accompanied by a gradient of the temperature.

The heat flux,  $\vec{Q}$ , in I, is related to the temperature gradient by  $\vec{Q} = -K \nabla T$ , where  $K$  is the thermal conductivity of the solution. Thus Eq. (7) relates the  $^3\text{He}$  density gradient to the heat flux by

$$\nabla n_3 = \frac{S_{ph} + n_3}{TK} \vec{Q}. \quad (8)$$

We see that the basic transport coefficient measured in I is the thermal conductivity. A second feature is the role of the  $^3\text{He}$  density. Since

$$S_{ph} = \frac{2\pi^2}{45} \left( \frac{T}{s} \right)^3 \quad (9)$$

one has

$$\frac{n_3}{S_{ph}} = 300 \frac{x_3}{T^3}, \quad (10)$$

with  $T$  measured in K; at  $T = 0.45$  K and  $x_3 = 3 \times 10^{-4}$  the ratio is unity.

## III. MICROSCOPIC SCATTERING PROCESSES

The microscopic processes that determine the transport properties of dilute solutions are  $^3\text{He}$ - $^3\text{He}$  [11], phonon-phonon [12], and phonon- $^3\text{He}$  [10] scatterings; the amplitudes of these processes are all well known from earlier helium research. At low energies, the total cross section for a  $^3\text{He}$  atom scattering from a second  $^3\text{He}$  atom of opposite spin can be written as

$$\sigma_{33} = \frac{9\pi^3}{k_D^2} v_{33,0}^2 \left( \frac{m^*}{m_4} \right)^2 \left( \frac{m_4 s}{k_D} \right)^4 = 10.3 \text{ \AA}^2, \quad (11)$$

where  $k_D$  is the Debye wave number, defined by  $n_4 = k_D^3/6\pi^2$ , and  $v_{33,0} = -0.064$  measures the strength of the  $^3\text{He}$ - $^3\text{He}$  interaction at zero momentum transfer [11]. Phonon-phonon scattering rates are rapid compared with phonon- $^3\text{He}$  rates. While such scatterings do not directly affect the heat current, they do play the important role of

keeping the phonon momentum distribution,  $n_{\vec{q}}$ , in local thermodynamic equilibrium with a drift velocity,  $\vec{v}_{ph}$ ,

$$n_{\vec{q}} = \frac{1}{e^{(sq - \vec{q} \cdot \vec{v}_{ph})/T} - 1}. \quad (12)$$

The amplitude for scattering of a phonon of wavevector  $\vec{q}$  against a  $^3\text{He}$  of wavevector  $\vec{p}$  to final states  $\vec{q}'$  and  $\vec{p}'$  is determined theoretically in terms of the measured excess volume,  $\alpha$ , of a  $^3\text{He}$  atom compared with that of a  $^4\text{He}$  atom and the  $^3\text{He}$  effective mass,  $m^*$ . To a first approximation the scattering is elastic, in the sense that  $q = q'$  and  $p = p'$ , with amplitude [10]

$$\langle p'q' | \mathcal{T} | pq \rangle = \frac{sq}{2n_4} (A + B \cos \theta), \quad (13)$$

where  $\theta$  is the angle between  $\vec{q}'$  and  $\vec{q}$ ,  $A = n_4 d\alpha/dn_4$  and  $B = (1 + \alpha + \delta m/m_4)(m_4/m^*)(1 + \alpha - m_3/m_4)$ . The momentum dependent scattering rate of phonons from the  $^3\text{He}$  is then

$$\gamma_3(q) = \frac{sq^4 x_3}{4\pi n_4} J, \quad (14)$$

where

$$J = A^2 + B^2/3 - 2AB/3; \quad (15)$$

the  $q^4$  in this rate is characteristic of Rayleigh scattering.

We estimate the importance of 3-3 versus phonon scattering in bringing the  $^3\text{He}$  into equilibrium. The mean free path of a  $^3\text{He}$  scattering on unpolarized  $^3\text{He}$  is

$$\ell_{33} = \frac{2}{n_3 \sigma_{33}} = \frac{8.66 \times 10^{-8}}{x_3} \text{cm}; \quad (16)$$

the factor  $n_3/2$  is the density of opposite spin  $^3\text{He}$ . Similarly, the mean free path for scattering of  $^3\text{He}$  of momentum  $p$  on phonons is given by  $p^3/m\Gamma$ , where

$$\begin{aligned} \Gamma &= \frac{1}{n_3} \int \frac{d^3q}{(2\pi)^3} q^2 \gamma_3(q) n_q^0 (1 + n_q^0) \\ &= 270\pi J \left( \frac{S_{ph}}{n_4} \right)^2 \frac{T^3}{s^2} \sim T^9, \end{aligned} \quad (17)$$

in the limit  $p \gg q$ . Here  $n_q^0 = (e^{sq/T} - 1)^{-1}$  is the equilibrium phonon distribution function. Replacing  $p^2$  by  $3m^*T$ , an appropriate thermal average, we find

$$\begin{aligned} \ell_{3ph} &= \frac{\sqrt{3}}{2J} \left( \frac{S_{ph}}{n_4} \right)^2 \frac{m^{*1/2} s^2}{T^{3/2}} \\ &= 0.077 \left( \frac{0.45 K}{T} \right)^{15/2} \text{cm}. \end{aligned} \quad (18)$$

Comparing the mean free paths (16) and (18), we find

$$\frac{\ell_{3ph}}{\ell_{33}} = 0.89 \times 10^6 x_3 \left( \frac{0.45 K}{T} \right)^{15/2}. \quad (19)$$

For  $T = 0.45\text{K}$  and  $x_3 = 10^{-6}$ ,  $\ell_{3ph} \approx \ell_{33}$ , while for  $T = 0.65\text{K}$  and  $x_3 = 3 \times 10^{-4}$ ,  $\ell_{3ph}/\ell_{33} \approx 16.9$ . Under the conditions of the experiment of I, a good first approximation is to assume that scattering of  $^3\text{He}$  by  $^3\text{He}$  atoms is fast compared with scattering of  $^3\text{He}$  by phonons. In fact, as will be shown in detail in [7], we may take the momentum distribution of the  $^3\text{He}$  to be simply that of a classical gas in equilibrium at rest,

$$f_p^0 = e^{-(p^2/2m^* - \mu_3)/T}. \quad (20)$$

#### IV. THERMAL CONDUCTIVITY

The thermal conductivity of the dilute solutions can in general be calculated by solving the coupled phonon and  $^3\text{He}$  Boltzmann equations to determine the steady state momentum distributions of the phonons and the  $^3\text{He}$ , and, from these distributions, the heat and particle currents. Since the phonon heat current density,  $\vec{Q}_{ph}$ , is nothing but the phonon momentum density times  $s^2$ ,

$$\vec{Q}_{ph} = s^2 \int \frac{d^3q}{(2\pi)^3} \vec{q} n_{\vec{q}} = T S_{ph} \vec{v}_{ph}, \quad (21)$$

where  $n_{\vec{q}}$  is the distribution of the phonons, the phonon thermal conductivity can be found simply under the conditions of the experiment in I by calculating the rate at which the phonons lose momentum by scattering against the stationary  $^3\text{He}$  [5, 6].

In a steady state the net force density on the phonons drifting at velocity  $\vec{v}_{ph}$  is balanced by the phonon pressure gradient,  $\nabla P_{ph} = S_{ph} \nabla T$ . Microscopically then,

$$\begin{aligned} \nabla P_{ph} &= - \int \frac{d^3q}{(2\pi)^3} \int \frac{d^3q'}{(2\pi)^3} \int 2 \frac{d^3p}{(2\pi)^3} \\ &\quad \times \vec{q} |\langle \mathcal{T} \rangle|^2 2\pi \delta(sq + p^2/2m^* - sq' - p'^2/2m^*) \\ &\quad \times [f_p^0 n_{\vec{q}} (1 + n_{\vec{q}'}) - f_{p'}^0 n_{\vec{q}'} (1 + n_{\vec{q}})], \end{aligned} \quad (22)$$

where  $\vec{p}' - \vec{p} = \vec{q} - \vec{q}' \equiv \vec{k}$ ,  $\langle \mathcal{T} \rangle = \langle p'q' | \mathcal{T} | pq \rangle$ , and the factor of 2 is from the  $^3\text{He}$  spin sum. In terms of the  $^3\text{He}$  structure function,

$$\begin{aligned} S_3(k, \omega) &= 2 \int \frac{d^3p}{(2\pi)^3} \delta(\omega + p^2/2m^* - p'^2/2m^*) f_p^0 \\ &= n_3 \left( \frac{m^*}{2\pi k^2 T} \right)^{1/2} e^{-m^*(\omega - k^2/2m^*)^2/2k^2 T}, \end{aligned} \quad (23)$$

which obeys  $S_3(k, -\omega) = e^{-\omega/T} S_3(k, \omega)$ , we can rewrite Eq. (22) as,

$$\begin{aligned} \nabla P_{ph} &= - \int \frac{d^3q}{(2\pi)^3} \int \frac{d^3q'}{(2\pi)^3} \int_{-\infty}^{\infty} d\omega \\ &\quad \times \vec{q} |\langle \mathcal{T} \rangle|^2 2\pi \delta(\omega - sq + sq') S_3(k, \omega) \\ &\quad \times [n_{\vec{q}} (1 + n_{\vec{q}'}) - n_{\vec{q}'} (1 + n_{\vec{q}}) e^{-\omega/T}]. \end{aligned} \quad (24)$$

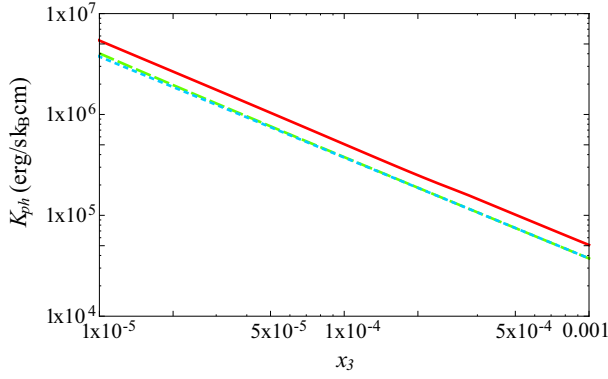


FIG. 1: (Color online) Thermal conductivity of a dilute solution of  $^3\text{He}$  in superfluid  $^4\text{He}$  at  $T = 0.45$  K. The approximate phonon thermal conductivity, Eq. (27) (dot-dashed line), in the limit in which the  $^3\text{He}$  are at rest in equilibrium is shown together with the full calculation from Ref. [7] (dashed line); these results differ only by a few percent at the lowest concentrations. The solid line shows the phonon thermal conductivity calculated with phonon recoil (see text).

Since  $n_{\vec{q}'}(1 + n_{\vec{q}}) = n_{\vec{q}}(1 + n_{\vec{q}'})e^{(\omega - \vec{k} \cdot \vec{v}_{ph})/T}$ , the final line in Eq. (24) to first order in  $v_{ph}$  is  $n_q^0(1 + n_{q'}^0)(\vec{k} \cdot \vec{v}_{ph})/T$ . Finally, symmetrizing the integrand in  $q$  and  $q'$ , and carrying out the angular averages, we have,

$$\nabla P_{ph} = -\frac{\vec{v}_{ph}}{6T} \int \frac{d^3q}{(2\pi)^3} \int \frac{d^3q'}{(2\pi)^3} n_q^0(1 + n_{q'}^0) k^2 |\langle \mathcal{T} \rangle|^2 \times \int_{-\infty}^{\infty} d\omega 2\pi \delta(\omega - sq + sq') S_3(k, \omega). \quad (25)$$

Neglecting  $^3\text{He}$  recoil is equivalent to setting  $S_3(k, \omega) = n_3 \delta(\omega)$ . In this case,

$$\begin{aligned} \nabla P_{ph} &= -\frac{\vec{v}_{ph}}{6T} \int \frac{d^3q}{(2\pi)^3} \int \frac{d^3q'}{(2\pi)^3} n_q^0(1 + n_{q'}^0) k^2 |\langle \mathcal{T} \rangle|^2 \\ &\quad \times 2\pi \delta(sq - sq'), \\ &= -\frac{n_3 \Gamma}{3T} \vec{v}_{ph} = -\frac{8\pi^5}{45} \frac{x_3 J}{n_4} \left(\frac{T}{s}\right)^8 \vec{v}_{ph}. \end{aligned} \quad (26)$$

Since  $\nabla P_{ph} = S_{ph} \nabla T$ , and  $\vec{Q}_{ph} = T S_{ph} \vec{v}_{ph} = -K_{ph} \nabla T$ , we conclude that

$$K_{ph} = \frac{3T^2 S_{ph}^2}{n_3 \Gamma} = \frac{n_4 s^2}{90\pi x_3 J T}. \quad (27)$$

Figure 1 shows the phonon thermal conductivity, using the parameters  $A = -1.2 \pm 0.2$  [13, 14], and  $B = 0.70 \pm 0.035$  [13–15]. The largest uncertainty is in  $A$ , owing to a systematic difference between the measurements [13, 14] of the pressure dependence of the density of dilute solutions. Numerically,  $J = 2.2 \pm 0.6$ .

As Bowley emphasized [6], allowing for the recoil of the  $^3\text{He}$  in scattering produces a significant correction to the effective phonon- $^3\text{He}$  scattering rate [17]. In Appendix A we describe the calculations in detail. These effects

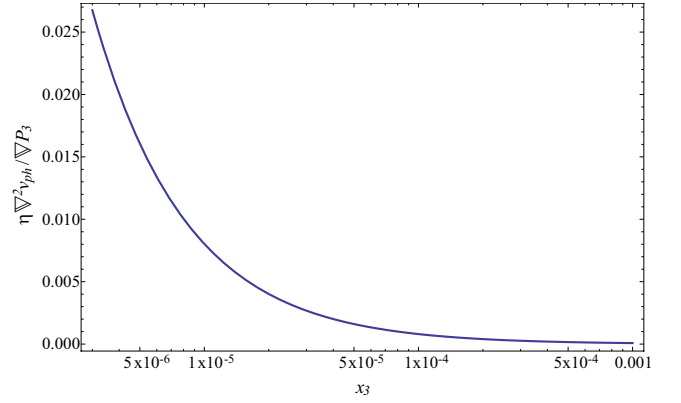


FIG. 2: Ratio of the contribution of the viscous term (see Eq. (4)) to the drag on the phonons due to scattering against the  $^3\text{He}$  at a temperature of 0.45 K. The magnitude of the drag is given by the  $^3\text{He}$  pressure gradient (see Eq. (26)) as a function of  $^3\text{He}$  concentration  $x_3$  (the concentrations measured in I are  $x_3 = 7 \times 10^{-5}$  and  $3 \times 10^{-4}$ ). The viscous term is calculated for laminar flow in a circular pipe of radius  $R = 2.5$  cm, using the  $^4\text{He}$  viscosity measured by Greywall [16].

increase the thermal conductivity by  $\sim 25 - 35\%$  in the range  $T = 0.45 - 0.65$  K (see Fig 1).

We return now to justify neglecting the phonon viscous stress in the pressure equation (4). The crucial question is the magnitude of this stress on the phonons compared with the drag they experience from scattering against the  $^3\text{He}$ , Eq. (25). We estimate the viscous stress, neglecting the drag, for laminar flow in a circular pipe of radius  $R$ , where  $\nabla^2 \vec{v}_{ph}$  is a constant,  $-8\langle \vec{v}_{ph} \rangle / R^2$ , throughout. As seen in Fig. 2, the ratio is well below 1%. In fact, the viscosity for flow in a circular pipe plays a role only in a thin boundary layer, which for the concentrations and temperatures of the experiment in I is of order mm thick.

## V. COMPARISON WITH EXPERIMENT

In the Lamoreaux et al. experiment, the heat flow produces a non-uniform temperature and  $^3\text{He}$  distribution, with the gradients of both  $T$  and  $n_3$  proportional to the inverse of the total thermal conductivity of the dilute solution, Eqs. (7) and (8). Note that the response of the  $^3\text{He}$  is proportional as well to  $S_{ph} + n_3$ . Since the  $^3\text{He}$  thermal conductivity is negligibly small throughout the range of concentrations in the experiment [owing to  $\ell_{33} \ll \ell_{3ph}$ , Eq. (19)], the experiment in fact measures the phonon thermal conductivity as limited by scattering against the  $^3\text{He}$ . In the calculation of the phonon thermal conductivity, deviations from the limit where  $^3\text{He}$ - $^3\text{He}$  scattering is dominant occur only at the lowest concentrations in the experiment and there only at a percent level.

The response of the  $^3\text{He}$  can be described in terms of the  $^3\text{He}$  diffusion constant,  $D_3$ , by noting that  $\nabla P_{ph} = -\nabla P_3$ , so that the relation between the phonon drift

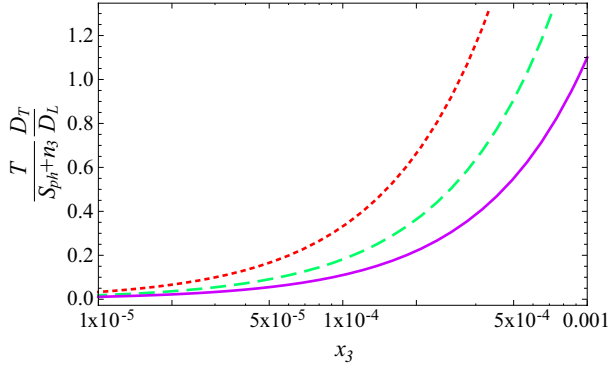


FIG. 3: (Color online) Contribution of the thermoelectric transport term relative to the effective diffusion constant,  $D_L$  extracted in I. The temperatures are 0.45 K (dotted), 0.55 K (dashed) and 0.65 K (solid).

and the phonon pressure gradient can be written as (cf. Eq. (25))

$$\frac{D_3}{T} \nabla P_3 = n_3 \vec{v}_{ph}, \quad (28)$$

where in the limit that the  $^3\text{He}$  are at rest in equilibrium,

$$D_3 = \frac{3T^2}{\Gamma}. \quad (29)$$

In the experimental situation, the phonon drift drives  $\nabla P_3$  rather than simply  $\nabla n_3$ . Equation (28) is, more generally, the response of the  $^3\text{He}$  current to the phonon wind [7],

$$\vec{j}_3 = n_3 \vec{v}_3 = n_3 v_{ph} - D_3 \nabla n_3 - D_T \nabla T, \quad (30)$$

in the situation where  $v_3 = 0$ . Here  $D_T = n_3 D_3 / T$  is an effective “thermoelectric” transport coefficient.

The analysis in I, in contrast, neglects the temperature gradient, and determines an effective diffusion constant,  $D_L$ , by setting a simplified expression for the  $^3\text{He}$  current to zero,

$$\vec{j}_{3L} \equiv n_3 \vec{v}_{ph} - D_L \nabla n_3 = 0, \quad (31)$$

(cf. Eq. (30)) thus defining  $D_L$ . Taking  $\vec{Q} = T S_{ph} \vec{v}_{ph}$ , Ref. I derives

$$\nabla n_3 = \frac{n_3}{T S_{ph} D_L} \vec{Q}. \quad (32)$$

To calculate  $D_L$  within our framework we compare Eq. (32) with Eq. (8) and find

$$D_L = \frac{n_3}{S_{ph} + n_3} \frac{K}{S_{ph}}. \quad (33)$$

We can also write  $D_L$  in terms of the general  $^3\text{He}$  transport coefficients as

$$D_L = D_3 - \frac{T}{S_{ph} + n_3} D_T = \frac{S_{ph}}{S_{ph} + n_3} D_3. \quad (34)$$

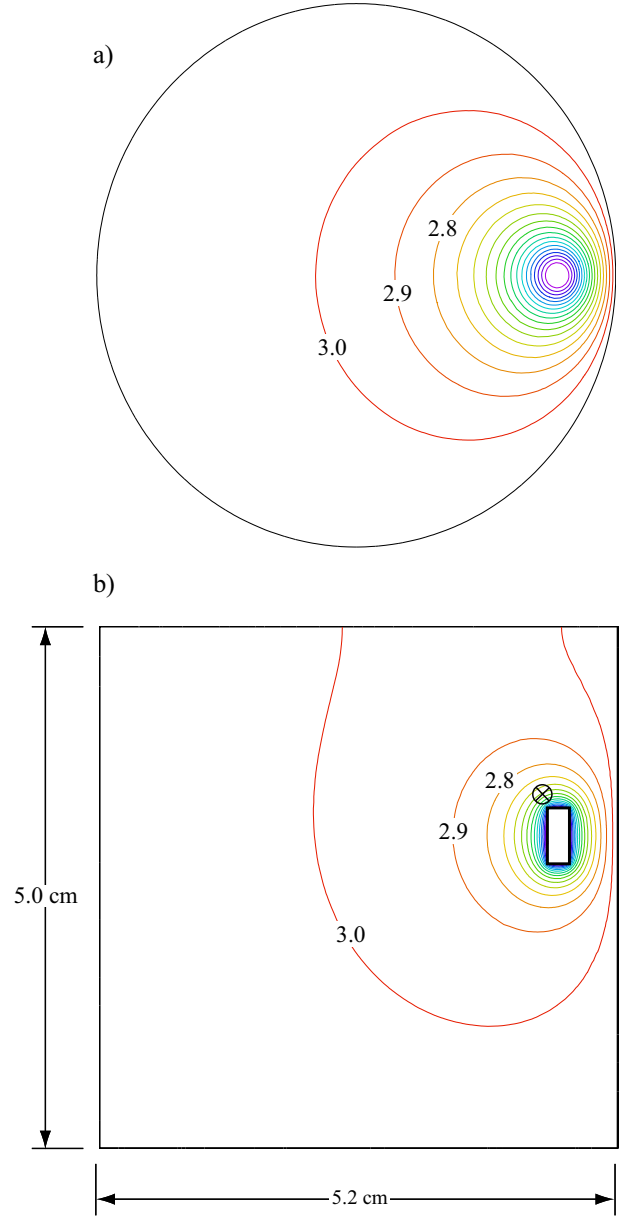


FIG. 4: (Color online) Example of the  $^3\text{He}$  distribution for a cell 5.2 cm in diameter and 5.0 cm high, with refrigerator temperature  $T_r = 0.45$  K, average  $x_3 = 3 \times 10^{-4}$ , and heater power 15 mW. The sections are: a) perpendicular to the cylinder axis and containing the neutron beam axis; and b) perpendicular to the neutron beam (the cross in the figure) and through the center of the heat source. We assume in this simulation that the cylindrical wall of the cell is at the same temperature as that of the base where the refrigerator is attached; the top surface is insulated. The  $^3\text{He}$  concentration contours, of constant spacing, are marked in units of  $10^{-4}$ ; the minimum is  $x_3 = 1.39 \times 10^{-4}$  at the surface of the heater and the maximum is  $3.03 \times 10^{-4}$  on the lower cell boundary.



The  $D_T$  term in this equation makes a significant contribution at higher concentrations (see Fig. 3); as noted,  $n_3 \sim S_{ph}$  for a significant part of the range of concentrations in I.

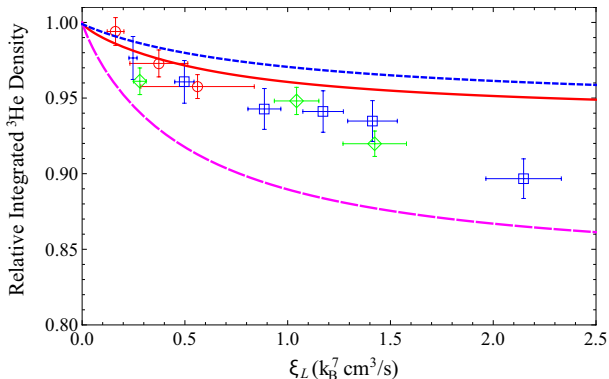


FIG. 5: (Color online) Representative results of the finite element calculation of the relative integrated  $^3\text{He}$  (column) density along the neutron beam as a function of the quantity  $\xi_L = T^7 \mathcal{P} / S_{ph} T$  where  $\mathcal{P}$  is the heater power, along with data from Ref. [3]. The curves are: *solid*,  $x_3 = 3 \times 10^{-4}$  and fixed refrigerator temperature  $T_r = 0.45$  K with the temperature of the cell barrel, the “conducting” boundary, also fixed at 0.45 K; *dashed*, the same calculation with only the refrigerator end at 0.45 K and the rest of the cell surface insulated; *dotted*,  $x_3 = 7 \times 10^{-5}$ ,  $T_r = 0.45$  K and the conducting boundary condition; the results for  $x_3 = 3 \times 10^{-4}$ ,  $T_r = 0.65$  K and the conducting boundary condition are, coincidentally, essentially the same as the dotted curve. The curves are plotted for the average temperature (greater than the boundary temperature) along the neutron beam path, resulting, at  $\xi_L = 2.5$ , in positive shifts of  $\xi_L$  ranging from  $\Delta\xi_L \approx 0.05 k_B^7 \text{ cm}^3/\text{s}$  for the solid curve to  $\Delta\xi_L \approx 0.5 k_B^7 \text{ cm}^3/\text{s}$  for the  $T = 0.65$  K case.

To further illustrate the physics, we now determine the  $^3\text{He}$  density distribution for several limiting cases in the geometry of the experiment in I [18]. There, the  $n_3$  distribution was determined by solving  $\nabla^2 v_{ph} = 0$  assuming constant temperature throughout the volume. Here we determine the  $n_3$  distribution by first writing

$$\nabla \cdot \vec{Q} = -\nabla \cdot (K_{ph} \nabla T) = -C \nabla \left( \frac{\nabla T}{P_3} \right) = 0, \quad (35)$$

where from Eq. (27),  $C = n_3^2 s^2 / 90 \pi J$ . We then eliminate  $P_3$  using the solution

$$P_3 + \frac{S_{ph} T}{4} = P, \quad (36)$$

of Eq. (6), where the constant  $P$  is the total pressure of the excitations. Equation (35) then reduces to a partial differential equation in  $T$  alone, which we solve using the finite element code FlexPDE. Given  $T(\vec{r})$  we then determine  $n_3(\vec{r})$  from Eq. (36), and determine the constant  $P$  by fixing the total number of  $^3\text{He}$  atoms in the system.

An example of the  $^3\text{He}$  distribution resulting from the finite element calculation is shown in Fig. 4; representative results of integrated  $^3\text{He}$  densities along the neutron beam are shown in Fig. 5 together with the data in Fig. 4 of I. The solution depends quite sensitively on whether one considers the barrel of the cylinder to be thermally conducting or insulating; calculations with these two assumptions bracket the data. To illustrate the effect of other variables in the problem, we also show in Fig. 5 the results for  $T = 0.65$  K and for the two concentrations used in I.

## VI. SUMMARY

We have analyzed the heat current and the resulting  $^3\text{He}$  spatial distribution in dilute solutions of  $^3\text{He}$  in superfluid  $^4\text{He}$  in the temperature range where phonons are the significant excitations of the  $^4\text{He}$ . We find that in the range of  $^3\text{He}$  concentrations in the Lamoreaux et al. experiment [3],  $7 \times 10^{-5} \leq x_3 \leq 3 \times 10^{-4}$ , heat transport is dominated by phonons. The response of the system is generally not a simple diffusion problem, described only by a  $^3\text{He}$  diffusion constant,  $D_3$ , since the temperature gradients are important. The experiment can be characterized as measuring the phonon thermal conductivity. A calculation of the  $^3\text{He}$  density along the neutron beam in the geometry of the experiment indicates that the well-tested microscopic theory of  $^3\text{He}$ -phonon scattering in dilute solutions of  $^3\text{He}$  in superfluid  $^4\text{He}$  is consistent with these results as well.

## Acknowledgments

This research was supported in part by NSF Grants PHY-0701611, PHY-0855569, PHY-0969790 and PHY-1205671. We thank Jen-Chieh Peng and Michael Hayden for helpful discussions about the experiment. Author GB is grateful to the Aspen Center for Physics, supported in part by NSF Grant PHY-1066292, and the Niels Bohr International Academy where parts of this research were carried out.

## Appendix A: Recoil corrections

In this Appendix we calculate contributions to the thermal conductivity due to the finite  $^3\text{He}$  mass. We start from Eq. (25) with the structure factor (23) of the  $^3\text{He}$ ,

$$\begin{aligned}
\nabla P_{ph} &= -\vec{v}_{ph} \frac{2\pi n_3}{6T} \int \frac{d^3 q}{(2\pi)^3} \int \frac{d^3 q'}{(2\pi)^3} n_q^0 (1 + n_{q'}^0) k^2 |\langle \mathcal{T} \rangle|^2 \left( \frac{m^*}{2\pi k^2 T} \right)^{1/2} e^{-m^*(sq - sq' - k^2/2m^*)^2/2k^2 T} \\
&= -\vec{v}_{ph} \frac{2\pi n_3}{6T} \int \frac{d^3 q}{(2\pi)^3} \int \frac{d^3 q'}{(2\pi)^3} \frac{k^2 |\langle \mathcal{T} \rangle|^2}{4 \sinh(sq/2T) \sinh(sq'/2T)} \left[ \left( \frac{m^*}{2\pi k^2 T} \right)^{1/2} e^{-m^*(sq - sq')^2/2k^2 T} \right] e^{-k^2/8m^* T}.
\end{aligned} \tag{A1}$$

The integral in Eq. (A1) is proportional to the inverse of the thermal conductivity. In the limit  $m^* \rightarrow \infty$  the expression in square brackets reduces to  $\delta(sq - sq')$ . For finite  $m^*$  there are two effects. First, the structure factor, and therefore also the scattering rate, is reduced in magnitude because of the nonzero momentum transfer,  $\vec{k} = \vec{q} - \vec{q}'$ , as is shown by the final Gaussian factor. Second, as the first Gaussian factor indicates, there is an energy transfer  $sq - sq'$  which is of order  $(Tk^2/m^*)^{1/2} \sim (T/m^* s^2)^{1/2} T$ .

The contributions to the scattering amplitude for nonzero energy transfer and for nonzero velocity of the

<sup>3</sup>He atoms have not been investigated in detail, although the basic processes were discussed in Ref. [10]. Here we make the simplest generalization of Eq. (13) that is symmetric under exchange of  $q$  and  $q'$ ,

$$\langle p'q' | \mathcal{T} | pq \rangle = \frac{s(qq')^{1/2}}{2n_4} (A + B \cos \theta). \tag{A2}$$

With prefactors omitted, the quantity to be calculated is thus

$$\int_0^\infty dq \int_0^\infty dq' \int_{-1}^1 d\cos \theta \frac{k(qq')^3 (A + B \cos \theta)^2}{4 \sinh(sq/2T) \sinh(sq'/2T)} e^{-m^* s^2 (q - q')^2/2k^2 T} e^{-k^2/8m^* T}. \tag{A3}$$

We have evaluated the integrals numerically and find, as stated in Sec. IV, that inclusion of recoil effects increases the thermal conductivity by  $\sim 25 - 35\%$  in the temperature range  $0.45 - 0.65$  K.

The leading corrections to the result for  $m^* \rightarrow \infty$  are of order  $T/m^* s^2$  relative to the result in the low temperature limit; we now calculate them analytically. To first order in  $T/m^* s^2$  the effects of the nonzero momentum transfer and the nonzero energy transfer are additive, and we calculate each in turn. The more important term is due to the momentum transfer. When this term alone is included one finds

$$\lim_{T \rightarrow 0} (TK)/TK \simeq 1 - \frac{1}{8m^* T} \frac{\langle k^4 \rangle}{\langle k^2 \rangle}, \tag{A4}$$

where

$$\langle \dots \rangle = \int_0^\infty dq \int_{-1}^1 d\cos \theta \frac{q^6 (A + B \cos \theta)^2}{4 \sinh^2(sq/2T)} (\dots). \tag{A5}$$

In these integrals we may replace  $k^2$  by its value  $2q^2(1 - \cos \theta)$  for zero energy transfer. The integrals over  $q$  and  $\theta$  decouple and one finds

$$TK \simeq \left( 1 + \frac{T}{4m^* s^2} \frac{\tilde{J}}{J} \frac{I_{10}}{I_8} \right) \lim_{T \rightarrow 0} (TK), \tag{A6}$$

where

$$\begin{aligned}
\tilde{J} &= \int_{-1}^1 \frac{d\cos \theta}{2} (A + B \cos \theta)^2 (1 - \cos \theta)^2 \\
&= \frac{4}{3} A^2 - \frac{4}{3} AB + \frac{8}{15} B^2
\end{aligned} \tag{A7}$$

and

$$I_n = \int_0^\infty dq \frac{x^n}{4 \sinh^2(x/2)} = n! \zeta(n), \tag{A8}$$

where  $\zeta(n)$  is the Riemann zeta function of order  $n$ . Therefore the thermal conductivity is given by

$$K \simeq \left( 1 + \frac{25\pi^2}{11} \frac{\tilde{J}}{J} \frac{T}{m^* s^2} \right) \frac{1}{T} \lim_{T \rightarrow 0} (TK). \tag{A9}$$

We now calculate the leading correction to the thermal conductivity due to the energy transfer, which is found by neglecting the term  $k^2/8m^* T$  in the exponent in Eq. (A3). The Gaussian in the energy difference has a width small compared with  $T$ , so we adopt a procedure similar to that used in making the Sommerfeld expansion for low temperature Fermi systems, where the derivative of the Fermi function approaches a delta function. In an

integral of the form,

$$G(x) = \int_0^\infty dy g(y) \frac{e^{-(x-y)^2/2\Delta^2}}{(2\pi\Delta)^{1/2}}, \quad (\text{A10})$$

where  $\Delta$  is a constant, and the function  $g(y)$  varies slowly on the scale  $\Delta$ , one finds on expanding  $g$  in a Taylor series

about  $y = x$ , that

$$G(x) = g(x) + \frac{\Delta^2}{2} g''(x) + \dots \quad (\text{A11})$$

When this result is applied to the  $q'$  integral in Eq. (A3) with the final Gaussian omitted, one finds

---


$$\begin{aligned} & \int_0^\infty dq \int_0^\infty dq' \int_{-1}^1 \frac{d\cos\theta}{2} \left( \frac{m^* s^2}{2\pi T k^2} \right)^{1/2} \frac{k^2 (qq')^3 (A + B \cos\theta)^2 e^{-m^* s^2 (q-q')^2 / 2k^2 T}}{4 \sinh^2(sq/2T)} \\ & \simeq J \int_0^\infty dq \frac{2q^8}{4 \sinh^2(sq/2T)} + \frac{T}{2m^* s^2} \int_0^\infty dq \int_{-1}^1 \frac{d\cos\theta}{2} \frac{k^2 q^3 k^2 (A + B \cos\theta)^2}{2 \sinh(sq/2T)} \left( \frac{\partial^2}{\partial(q')^2} \frac{k^2 q'^3}{2 \sinh(sq'/2T)} \right)_{q'=q}, \end{aligned} \quad (\text{A12})$$

which, when expressed in terms of the variables  $x = sq/T$ ,  $y = sq'/T$ , and  $z = \cos\theta$ , is proportional to

$$J \int_0^\infty dx \frac{2x^8}{4 \sinh^2(x/2)} + \frac{T}{m^* s^2} \int_0^\infty dx \frac{x^5}{2 \sinh(x/2)} \int_{-1}^1 \frac{dz}{2} (1-z)(A+Bz)^2 \left( \frac{\partial^2}{\partial y^2} \frac{\kappa^2 y^3}{2 \sinh(y/2)} \right)_{y=x}, \quad (\text{A13})$$

where  $\kappa^2 = x^2 + y^2 - 2xyz$ . The second derivative is

$$\frac{x^3}{\sinh(x/2)} \left\{ 1 + (1-z) \left[ 12 - \frac{1}{4}x^2 - 4x \coth(x/2) + \frac{1}{2}x^2 \coth^2(x/2) \right] \right\}. \quad (\text{A14})$$


---

On evaluating the integrals, one finds that the effect of energy transfer produces contributions to the integral (A3) having the form

$$1 + \left( 1 - \frac{(25\pi^2 - 198)\tilde{J}}{33J} \right) \frac{T}{m^* s^2}. \quad (\text{A15})$$

The numerical factor  $(25\pi^2 - 198)/33$  is approximately 1.477 and thus one sees that the effects of nonzero energy transfer are much less important than those due to nonzero momentum transfer. When both contributions to the thermal conductivity are included, one finds on inserting Eq. (27) for the low temperature limiting behavior,

$$K \simeq \frac{n_4 s^2}{90\pi x_3 J T} \left( 1 + \frac{T}{m^* s^2} \left[ \frac{100\pi^2 - 198}{33} \frac{\tilde{J}}{J} - 1 \right] \right). \quad (\text{A16})$$


---

The coefficient of  $\tilde{J}/J$  is approximately 23.90. For  $A = -1.2$  and  $B = 0.70$ ,  $J$  is 2.16,  $\tilde{J}$  is 3.30 and their ratio is 1.52. Thus the coefficient of  $T/m^* s^2$  is 35.5. Even though  $m^* s^2 = 48.1$  K, the effects of recoil are large even at temperatures well below 1 K as a consequence of the large numerical coefficient. This coefficient reflects the fact that the most important contributions to the momentum transfer arise from phonons with momenta  $\gg T/s$ . At  $T = 0.5$  K the correction is 37%, which is considerable. Higher-order contributions in  $T$  can be significant, and one would expect these to reduce the deviation from the low-temperature limiting result by an amount of relative order  $(0.37)^2 \sim 10\%$ . These analytic results are in good agreement with the numerical integration of Eq. (A3) described above, and shown in Fig. 1.

- [1] R. Golub and S. K. Lamoreaux, Phys. Rep. **237**, 1 (1994).
- [2] M. Hayden, S. K. Lamoreaux, and R. Golub, AIP Conf. Proc. **850**, 147 (2006).
- [3] S. K. Lamoreaux, G. Archibald, P. D. Barnes, W. T. Buttlar, D. J. Clark, M. D. Cooper, M. Espy, G. L. Greene, R. Golub, M. E. Hayden, C. Lei, L. J. Marek, J.-C. Peng, and S. Penttila, Europhys. Lett. **58**, 718 (2002).

- [4] G. Baym and C. J. Pethick, *Landau Fermi liquid theory: concepts and applications*, (J. Wiley and Sons, 1991), and references therein.
- [5] G. Baym, R. G. Barrera, and C. J. Pethick, Phys. Rev. Letters **22**, 20 (1969).
- [6] R. M. Bowley, Europhys. Lett. **58**, 725 (2002).
- [7] G. Baym, D. H. Beck, and C. J. Pethick, to be published.



- [8] G. Baym, D. H. Beck, and C. J. Pethick, to be published.
- [9] The phonon contributions to the dissipative second viscosity terms in the superfluid acceleration equation vanish, see I. M. Khalatnikov, *Introduction to the Theory of Superfluidity*, (W. A. Benjamin, New York, 1965), pp. 65,133.
- [10] G. Baym and C. Ebner, Phys. Rev. **164**, 235 (1967).
- [11] G. Baym and C. Ebner, Phys. Rev. **170**, 346 (1968).
- [12] H. J. Maris, Rev. Mod. Phys. **49**, 341 (1977).
- [13] C. Boghosian and H. Meyer, Phys. Lett. **A25**, 352 (1967).
- [14] G. E. Watson, J. D. Reppy, and R. C. Richardson, Phys. Rev. **188**, 384 (1969).
- [15] B. M. Abraham, C. G. Brandt, Y. Eckstein, J. Munarin, and G. Baym, Phys. Rev. **188**, 309 (1969).
- [16] D. S. Greywall, Phys. Rev. B **23**, 2152 (1981).
- [17] Note that in the implementation of this correction in Ref. [6], the  $^3\text{He}$  effective mass is taken to be one third of its actual value, and therefore the effects of recoil are overestimated.
- [18] We are grateful to M. Hayden, private communication, for the geometric details.